Direct Phase Measurement Interferometry and Optical Testing

- Phase-Stepping and Phase-Shifting
  - –Basic Concept
  - –Phase Shifters
  - –Algorithms
  - –Phase-unwrapping
  - –Phase shifter calibration
  - –Errors
- Spatial synchronous and Fourier methods
- Solving vibration problems
- Multiple wavelength and vertical scanning (Coherence Probe) techniques

Advantages of Phase-Shifting Interferometry

- High measurement accuracy (>1/1000 fringe, fringe following only 1/10 fringe)
- Rapid measurement
- Good results with low contrast fringes
- Results independent of intensity variations across pupil
- Phase obtained at fixed grid of points
- Easy to use with large solid-state detector arrays

Phase Shifting Interferometry

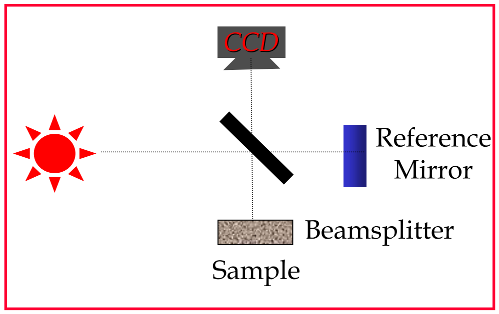

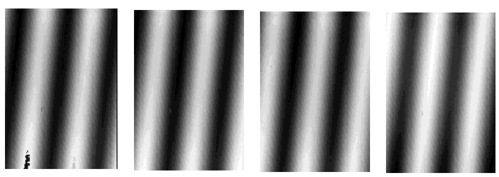

90° phase shift
between measurements

Phase Shifting - Moving Mirror

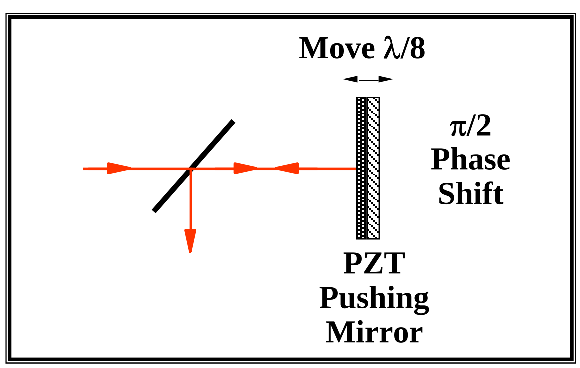

Phase Shifting - Diffraction Grating

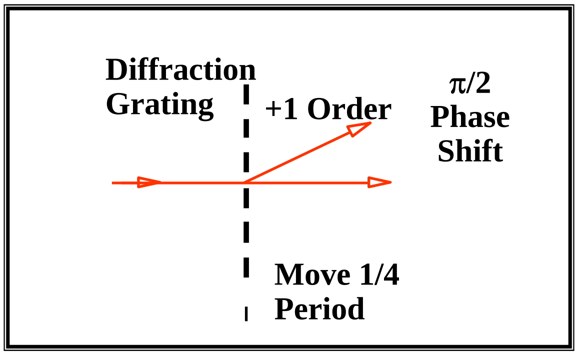

Phase Shifting - Bragg Cell

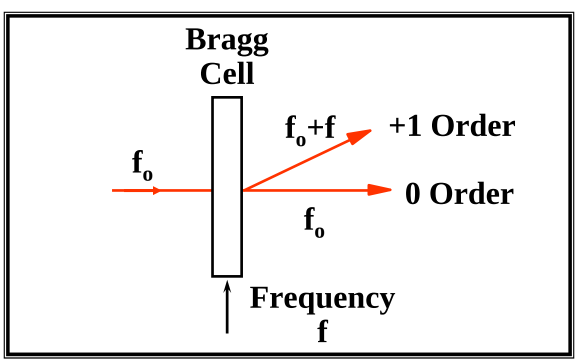

Phase Shifting - Rotating Half-Wave Plate

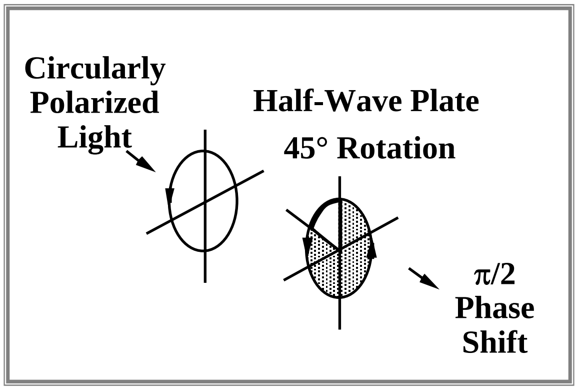

Geometric Phase Shifter 1

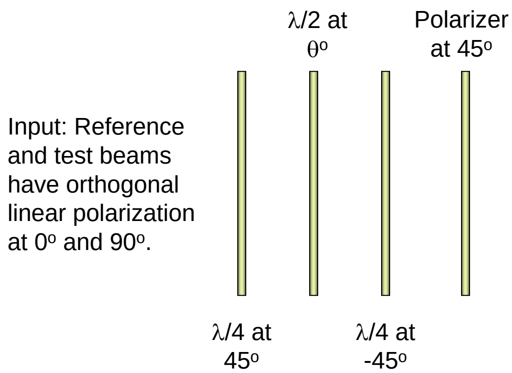

If the half-wave plate is rotated an angle θ the phase difference between the test and reference beams changes by 4θ.

Geometric Phase Shifter 2

Input: Reference and test beams have orthogonal linear polarization at 0^o and 90^o.

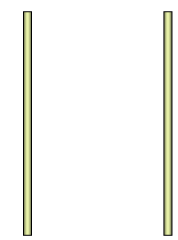

If the polarizer is rotated an angle θ the phase difference between the test and reference beams changes by 2θ.

Zeeman Laser

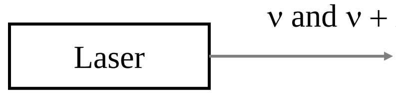

Two frequencies have orthogonal polarization

Frequency Shifting Source

Phase = $(2\pi/\lambda)$ (path difference) = $(2\pi/c)\,\nu$ (path difference)

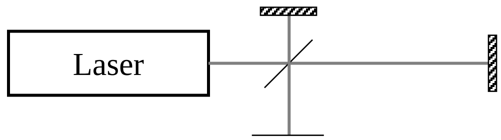

Phase shift = $(2\pi/c)$ (frequency shift) (path difference)

Four Step Method

$$I(x,y) = I_{dc} + I_{ac}\cos[\phi(x,y) + \phi(t)]$$

phase shift: $\phi(t)$

measured object phase: $\phi(x,y)$

$\mathbf{I_1(x,y) = I_{dc} + I_{ac}}\cos[\phi(x,y)]$	$\phi(t) = 0$ (0°)
$\mathbf{I_2(x,y) = I_{dc} - I_{ac}}\sin[\phi(x,y)]$	$= \pi/2$ (90°)
$\mathbf{I_3(x,y) = I_{dc} - I_{ac}}\cos[\phi(x,y)]$	$= \pi$ (180°)
$\mathbf{I_4(x,y) = I_{dc} + I_{ac}}\sin[\phi(x,y)]$	$= 3\pi/2$ (270°)

$$\mathrm{Tan}[\phi(\mathbf{x},\mathbf{y})] = \frac{\mathbf{I}_4(\mathbf{x},\mathbf{y}) - \mathbf{I}_2(\mathbf{x},\mathbf{y})}{\mathbf{I}_1(\mathbf{x},\mathbf{y}) - \mathbf{I}_3(\mathbf{x},\mathbf{y})}$$

Relationship Between Phase Heights

$$\phi(\mathrm{x,y}) = \mathrm{Tan}^{-1}\left[\frac{I_4(x,y) - I_2(x,y)}{I_1(x,y) - I_3(x,y)}\right]$$

$$\mathrm{Height}(x,y) = \frac{\lambda}{4\pi}\phi(x,y)$$

Phase-measurement Algorithms

Three Measurements $\phi = \tan^{-1}\left[\frac{I_3 - I_2}{I_1 - I_2}\right]$

Four Measurements $\phi = \tan^{-1}\left[\frac{I_4 - I_2}{I_1 - I_3}\right]$

Schwider-Hariharan Five Measurements $\phi = \tan^{-1}\left[\frac{2(I_2 - I_4)}{2I_3 - I_5 - I_1}\right]$

Carré Equation

$$\phi = \tan^{-1}\left[\frac{\sqrt{[3(I_2 - I_3) - (I_1 - I_4)][(I_2 - I_3) - (I_1 - I_4)]}}{(I_2 + I_3) - (I_1 + I_4)}\right]$$

Phase-Stepping Phase Measurement

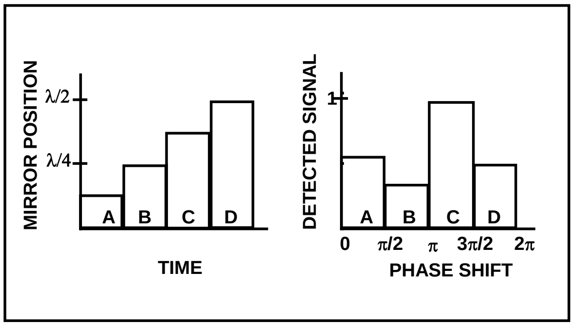

Integrated-Bucket Phase Measurement

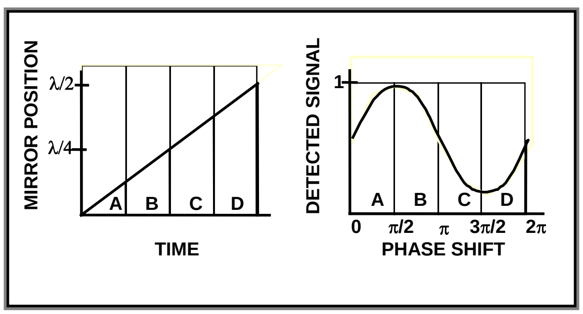

Integrating-Bucket and Phase-Stepping Interferometry

Measured irradiance given by

$$I_i = \frac{1}{\Delta}\int_{\alpha_i-\Delta/2}^{\alpha_i+\Delta/2} I_o\left\{1+\gamma_o\cos[\phi+\alpha_i(t)]\right\}d\alpha(t)$$

$$= I_o\left\{1+\gamma_o \text{sinc}\left[\frac{\Delta}{2}\right]\cos[\phi+\alpha_i]\right\}$$

Integrating-Bucket $\Delta=\alpha$

Phase-Stepping $\Delta=0$

Typical Fringes For Spherical Surfaces

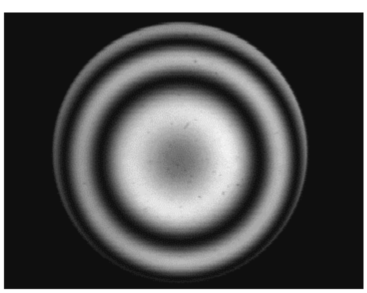

Fringes

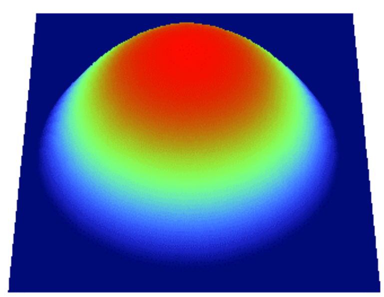

Phase map

Phase Ambiguities

-Before Unwrapping

2 π Phase Steps

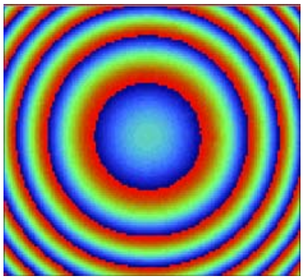

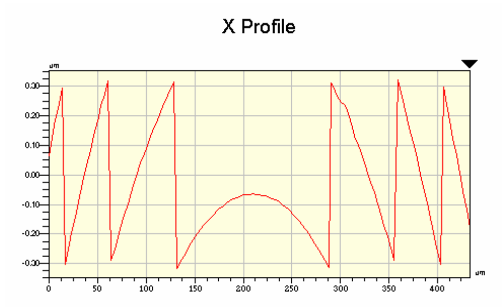

Phase Multiple Solutions

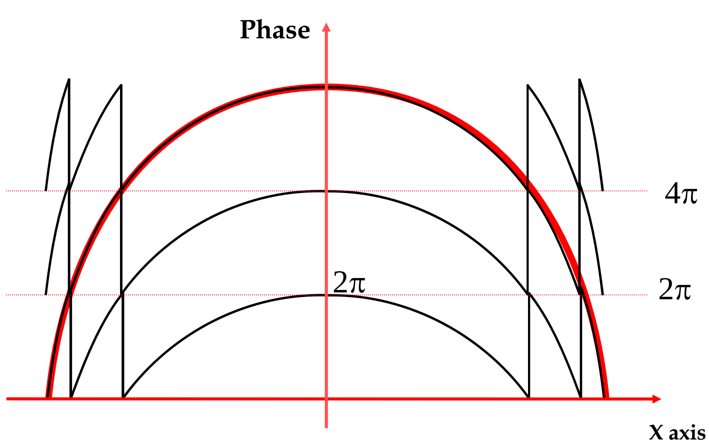

Removing Phase Ambiguities

- Arctan Mod 2π (Mod 1 wave)
- Require adjacent pixels less than π difference

  (1/2 wave OPD)

- Trace path
- When phase jumps by > π

  Add or subtract N2π

  Adjust so < π

Phase Ambiguities - After Unwrapping

Phase Steps Removed

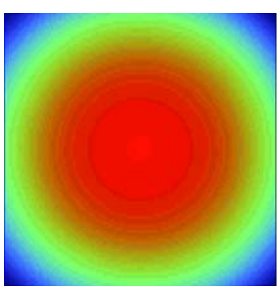

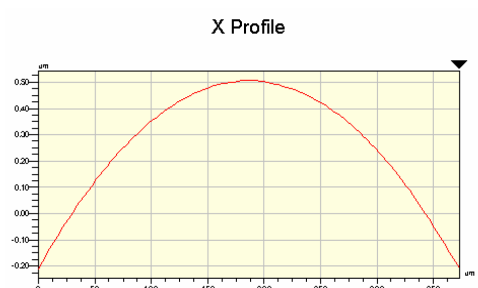

Phase-Shifting Interferometer

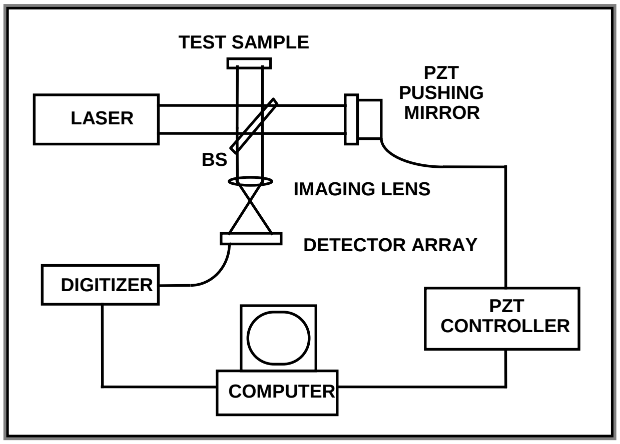

Phase Shifter Calibration

Let the phase shifts be -2α, -α, 0, α, 2α

$$\alpha = ArcCos\left(\frac{1}{2}\frac{I_5(x,y)-I_1(x,y)}{I_4(x,y)-I_2(x,y)}\right)$$

A limitation of this algorithm is that there are singularities for certain values of the wavefront phase. To avoid errors, a few tilt fringes are introduced into the interferogram and data points for which the numerator or denominator is smaller than a threshold are eliminated.

It is often convenient to look at a histogram of the phase shifts. If the histogram is wider than some preselected value it is known that there must be problems with the system such as too much vibration present.

Error Sources

- **Incorrect phase shift between data frames**
- **Vibrations**
- **Detector non-linearity**
- **Stray reflections**
- **Quantization errors**
- **Frequency stability**
- **Intensity fluctuations**

RMS Repeatability

Definition:

Take two frames of data and subtract the two frames point by point to determine rms of difference.

RMS surface height repeatability $\lambda/1000$.
(assuming good environment)

Averaging improves repeatability.

Repeatability generally limited by environment, rather than interferometer.

Four π/2 Steps

Phase error due to 5% phase shift calibration error.

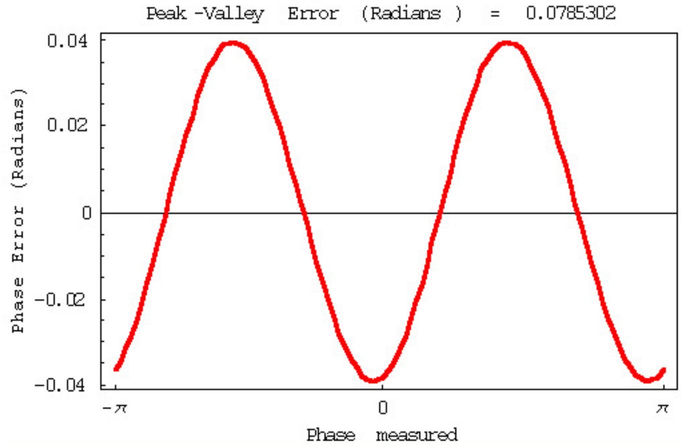

Phase Error Compensating Techniques

Two data sets with π/2 phase shift.

- Calculate a phase for each set from algorithm, and then average phases.
- Average Numerator and Denominator, and then calculate phase.

Example of Algorithm Derivation

Averaging Technique

4-FRAME (offset = 0)

frames # 1,2,3,4

$$\frac{I_4 - I_2}{I_1 - I_3} = \frac{N_1}{D_1}$$

4-FRAME (offset = $\pi/2$)

frames# 2,3,4,5

$$\frac{I_4 - I_2}{I_5 - I_3} = \frac{N_2}{D_2}$$

5-FRAME

$$\tan\varphi = \frac{N_1 + N_2}{D_1 + D_2} = \frac{2(I_4 - I_2)}{I_1 + I_5 - 2I_3}$$

Schwider-Hariharan Five $\pi/2$ Step Algorithm

- Error of same double-frequency form as for 4-step algorithm, but magnitude of error reduced by a factor of more than 25.

Error due to detector nonlinearity

- Generally CCD's have extremely linear response to irradiance
- Sometimes electronics between detector and digitizing electronics introduce nonlinearity
- Detector nonlinearity not problem in well designed system.
- Schwider-Hariharan algorithm has no error due to 2^{nd} order nonlinearity. Small error due to 3^{rd} order.

Error due to Stray Reflections

- Stray reflections in laser source interferometers introduce extraneous interference fringes.
- Stray reflections add to test beam to give a new beam of some amplitude and phase.
- Difference between this resulting phase and phase of test beam gives the phase error.

Error – Stray Reflections

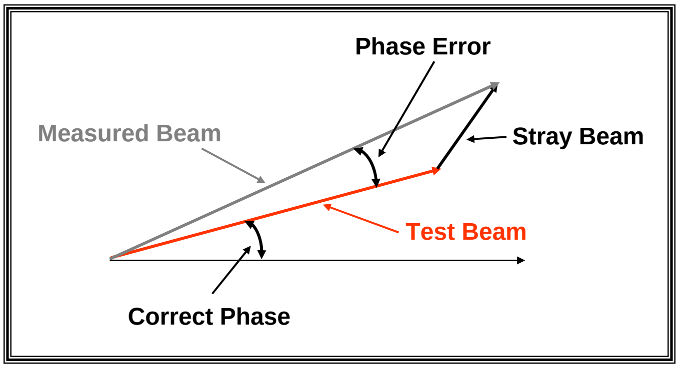

Quantization Error

rms phase error = $\frac{1}{\sqrt{3}\ 2^{N}}$ N = number of bits

N	6	8	10	12
Phase error	9.0E-3	2.3E-3	5.6E-4	1.4E-4
Fringes	1.4E-3	3.6E-4	9.0E-5	2.2E-5
Surface error	4.54	1.14	0.28	0.07
(Angstroms)				

Averaging further reduces error.

Reference: Chris Brophy, J. Opt. Soc. Am. A, **7**, 537-541 (1990).

5.6 Spatial Synchronous and Fourier Methods

Both techniques use a single interferogram having a large amount of tilt.

The interference signal is given by

```
irradiance[x_, y_] := iavg (1 + γ Cos[ϕ[x, y] + 2 π f x])
```

Spatial Synchronous

The interference signal is compared to reference sinusoidal and cosinusoidal signals.

The two reference signals are

```
rcos[x_, y_] := Cos[2 π f x]
```

and

```
rsin[x_, y_] := Sin[2 π f x]
```

Multiplying the reference signal times the irradiance signal gives sum and difference signals.

```
TrigReduce[irradiance[x, y] rcos[x, y]]
```

$$\frac{1}{2}\,(2\,\text{iavg}\,\text{Cos}[2\,f\,\pi\,x] + \text{iavg}\,\gamma\,\text{Cos}[\phi[x, y]] + \text{iavg}\,\gamma\,\text{Cos}[4\,f\,\pi\,x + \phi[x, y]])$$

```
TrigReduce[irradiance[x, y] rsin[x, y]]
```

$$\frac{1}{2}\,(2\,\text{iavg}\,\text{Sin}[2\,f\,\pi\,x] - \text{iavg}\,\gamma\,\text{Sin}[\phi[x, y]] + \text{iavg}\,\gamma\,\text{Sin}[4\,f\,\pi\,x + \phi[x, y]])$$

The low frequency second term in the two signals can be written as

$$s1 = \frac{\text{iavg}\,\gamma}{2}\,\text{Cos}[\phi[x, y]]$$

$$s2 = -\frac{\text{iavg}\,\gamma}{2}\,\text{Sin}[\phi[x, y]]$$

$$\text{Tan}[\phi[x, y]] = \frac{-s2}{s1}$$

The only effect of having the frequency of the reference signals slightly different from the average frequency of the interference signal is to introduce tilt into the final calculated phase distribution.

Fourier Method

The interference signal is Fourier transformed, spatially filtered, and the inverse Fourier transform of the filtered signal is performed to yield the wavefront.

The Fourier analysis method is essentially identical to the spatial synchronous method. The irradiance can be written as

$$\text{irradiance}[x, y] = \text{iavg}\,(1 + \gamma\,\text{Cos}[\phi[x, y] + 2\,\pi\,f\,x])$$

We can rewrite this as

$$\text{irradiance}[x, y] = \text{iavg}\left(1 + \frac{1}{2}\,e^{-2\,i\,f\,\pi\,x - i\,\phi[x,y]}\,\gamma + \frac{1}{2}\,e^{2\,i\,f\,\pi\,x + i\,\phi[x,y]}\,\gamma\right)$$

We can take the Fourier transform of this irradiance signal and spatially filter to select the portion of the Fourier transform around the spatial frequency f, and then take the inverse Fourier transform of this filtered signal to give the wavefront.

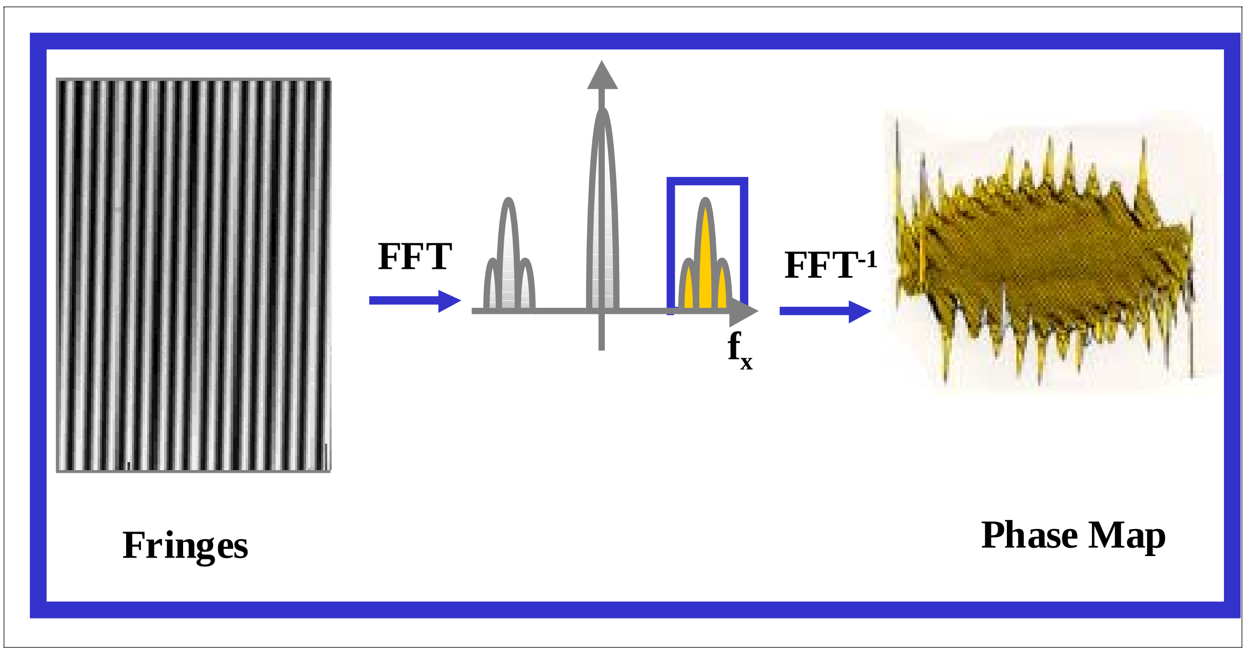

Note that both the spatial synchronous method and the Fourier method require a large amount of tilt be introduced to separate the orders. Since a spatially limited system is not band limited, the orders are never completely separated and the resulting wavefront will always have some ringing at the edges. Also, the requirement for large tilt always limits the accuracy of the measurement. The advantage of the techniques is that only a single interferogram is required and vibration and turbulence cause less trouble than if multiple interferograms were required.

Error Due to Vibration

- Probably the most serious impediment to wider use of PSI is its sensitivity to external vibrations.
- Vibrations cause incorrect phase shifts between data frames.
- Error depends upon frequency of vibration present as well as phase of vibration relative to the phase shifting.

Best Way to Fix Vibration Problem

- Retrieve frames faster
- Control environment
- Common-path interferometers
- Measure vibration and introduce vibration 180 degrees out of phase to cancel vibration
- Grab all frames at once (Single Shot)
- Carrier Frequency
- Pixelated Array

Vibration Compensation Concept

- **Example: Twyman-Green configuration**
  - **Sense optical phase**
  - **Feed back out-of-phase signal to phase shifter**

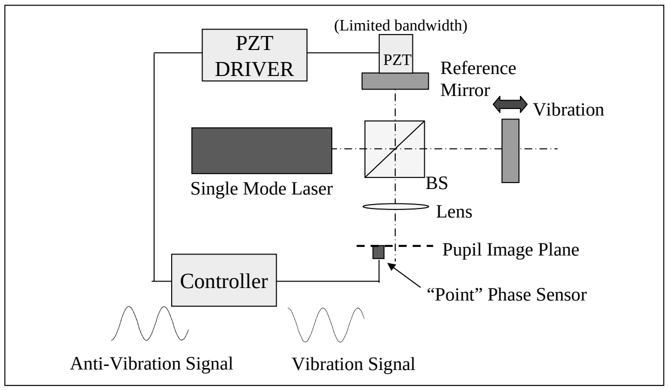

Achieving High Speed Phase Modulation

- **Use polarization Twyman-Green configuration**
- **EOM changes relative phase between 'S' & 'P' components**
  - **Can be very fast: 200 kHz - 1 GHz response**

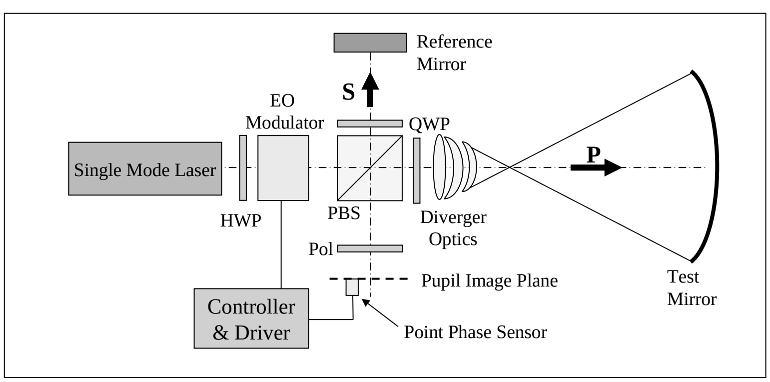

Results

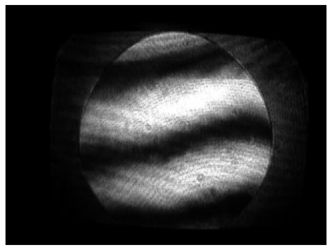

Conclusions - Active Vibration Cancellation Interferometer

System works amazingly well, but it is rather complicated and expensive.

Simultaneous Phase-Measurement Interferometer

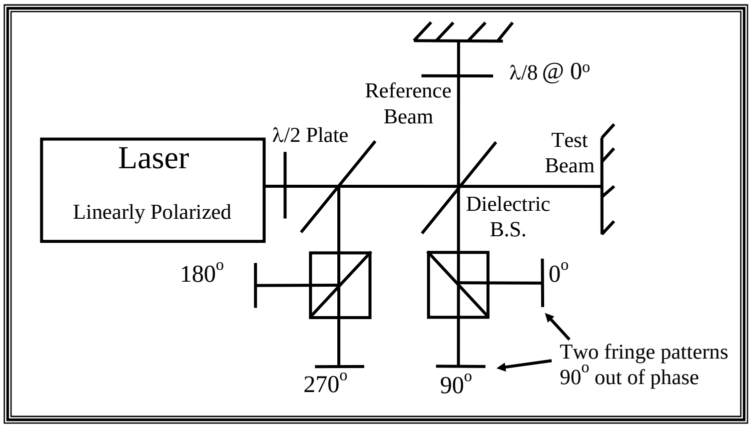

Dielectric beamsplitter and phase shift upon reflection for test and reference beams

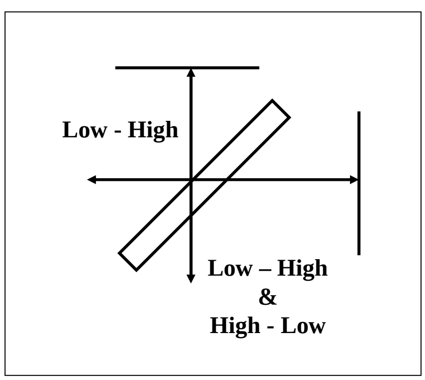

4D PhaseCam Operation

- **Twyman-Green**
  - **Two beams have orthogonal polarization**
- **4 Images formed**
  - **Holographic element**
- **Single Camera**
  - **1024 x 1024**
  - **2048 x 2048**
- **Polarization used to produce 90-deg phase shifts**

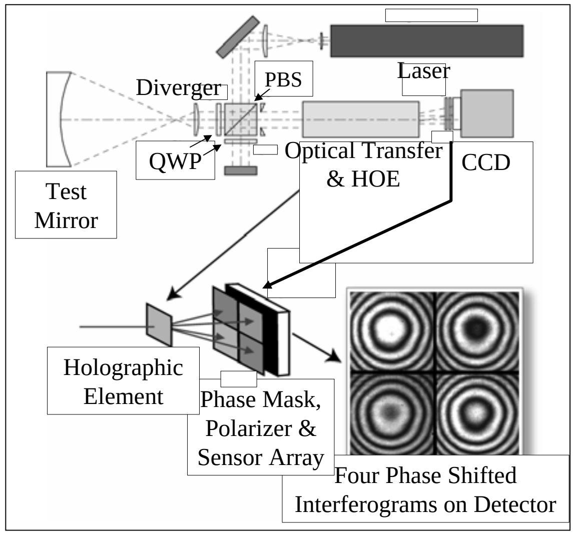

Effects of Vibration

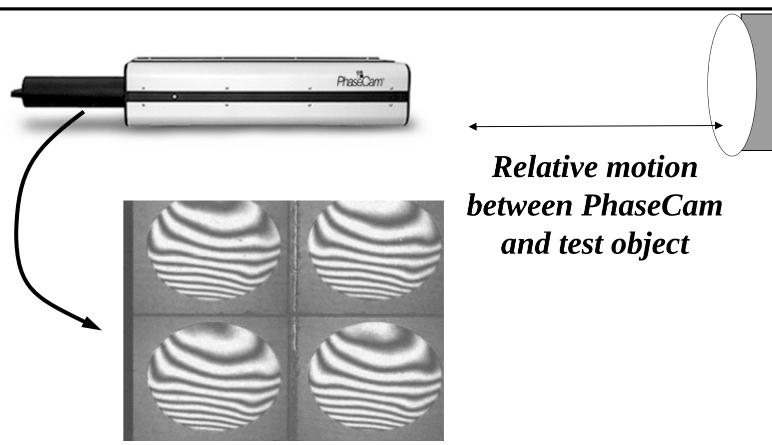

Phase relationship is fixed

Testing a 0.5 meter diameter, 20 meter ROC mirror

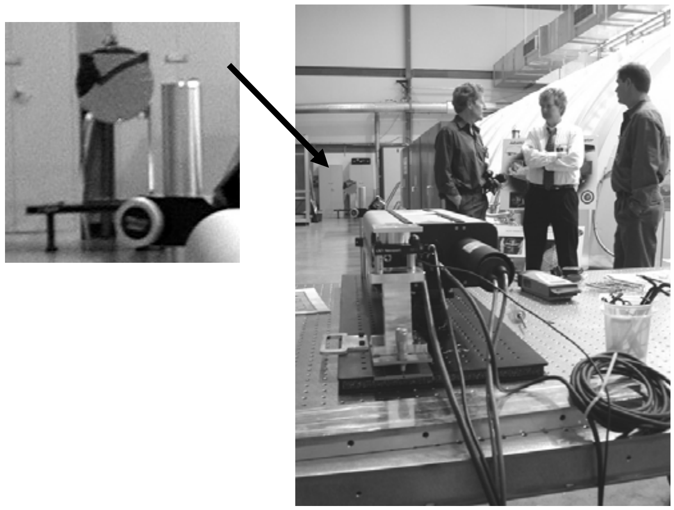

0.5 m diameter mirror, 20 m ROC 5 nm rms repeatability (in air)

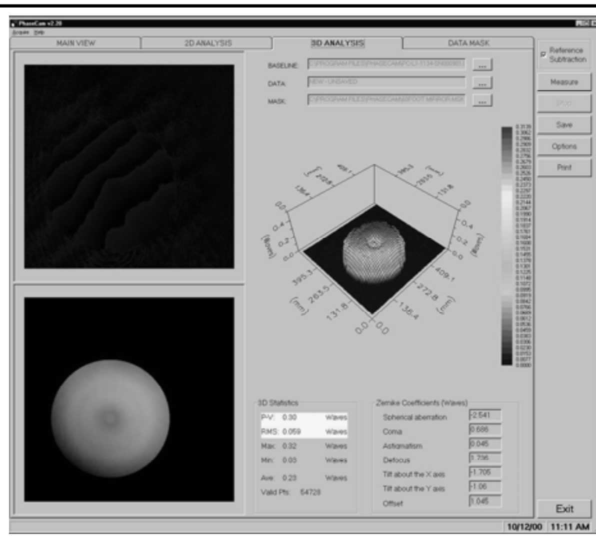

Phase Sweep at 408 Hz

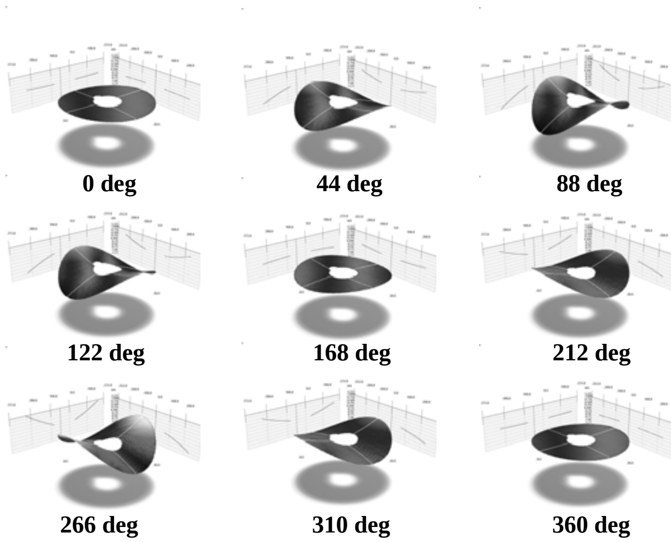

Hard Disk Platter Excited by PZT at 408 Hz

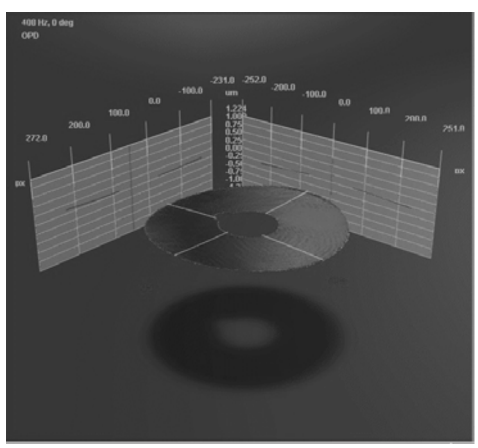

Hard Disk Platter Excited by PZT at 3069 Hz

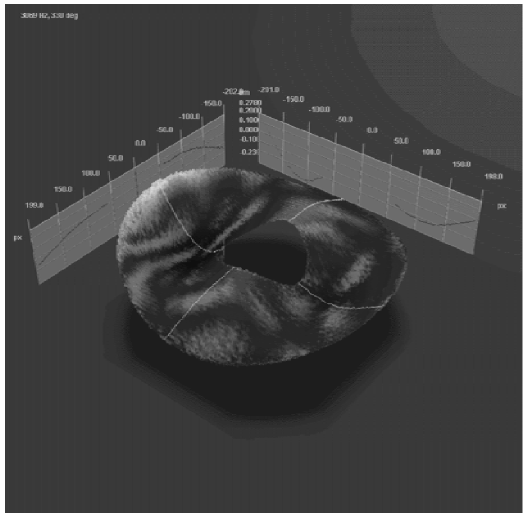

Surface Subtraction

Subtraction in interferogram domain (diffuse and specular surfaces)

Stetson - 8 frame phase-difference

$$\Delta Z = \frac{\lambda}{2}\,\mathrm{atan}\left(\frac{[D_0 - B_0][A(t)-C(t)]-[A_0 - C_0][D(t)-B(t)]}{[A(t)-C(t)][A_0 - C_0]+[D_0 - B_0][D(t)-B(t)]}\right)$$

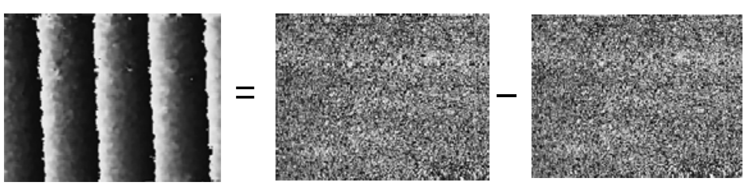

+ Unwrapping **A(t),B(t),C(t),D(t)** **A_0,B_0,C_0,D_0**

• ***Not necessary to solve for random phase***

Backplane Deformation Holder

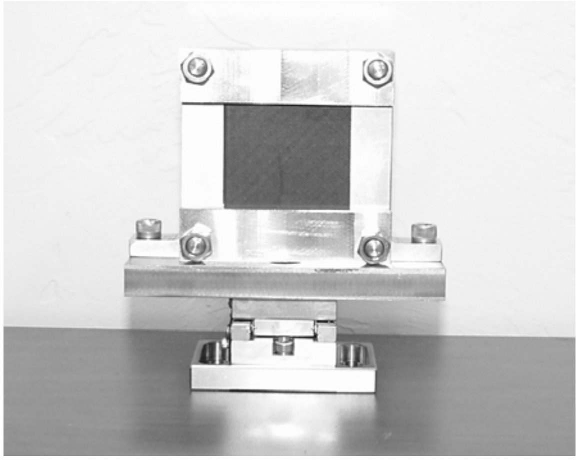

Set Up for Backplane Deformation Measurement

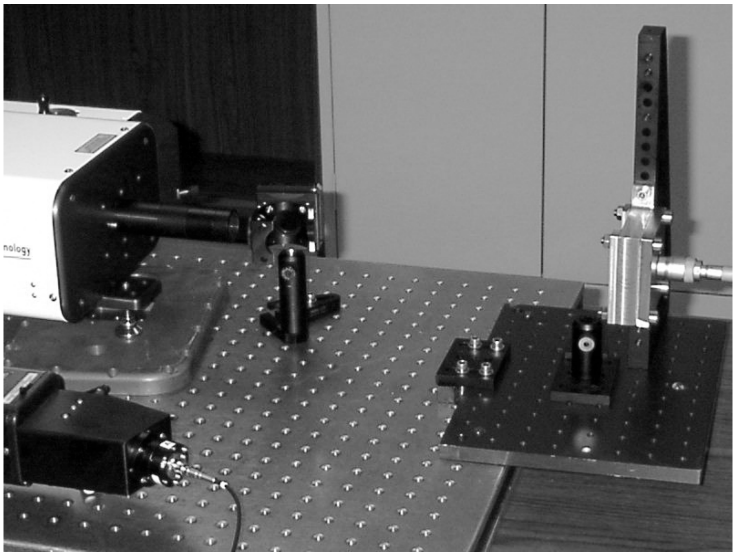

Backplane

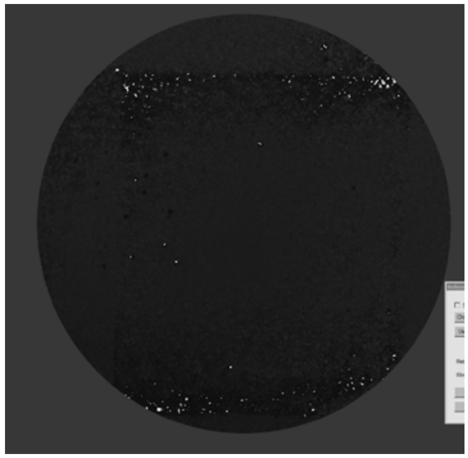

Carbon Fiber Deformation

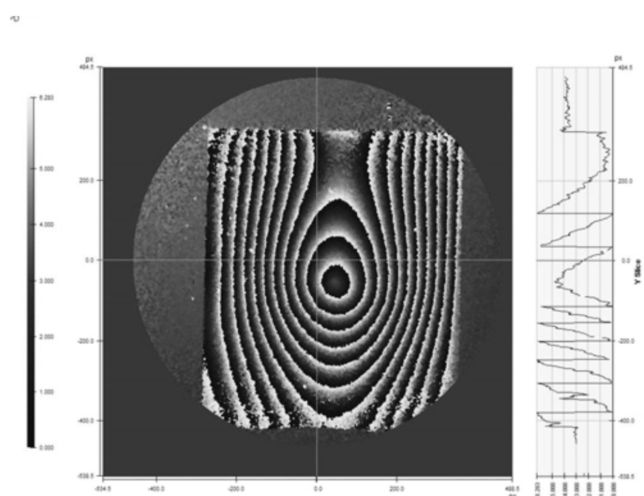

(Metrology for JWST Backplane)

Conclusions – Single Shot Interferometer

- Vibration insensitive, quantitative interferometer
- Surface figure measurement (nm resolution)
- Snap shot of surface height
- Acquisition of "phase movies"

Still not perfect

Not easy to use multiple wavelength or white light interferometry

N-Point Technique (Carrier Frequency)

Phase shifting algorithms applied to consecutive pixels thus requires calibrated tilt

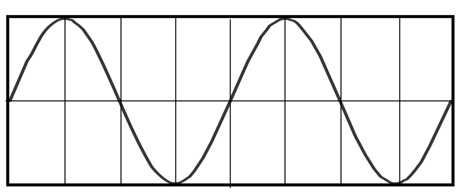

4 pixels per fringe for 90 degree phase shift

Creating the Carrier Frequency

- **Introduce tilt in reference beam**
  - Aberrations introduced due to beam transmitting through interferometer off-axis
- **Wollaston prism in output beam**
  - Requires reference and test beams having orthogonal polarization
- **Pixelated array in front of detector**
  - Special array must be fabricated

Use of Wollaston Prism to Produce Carrier Fringes

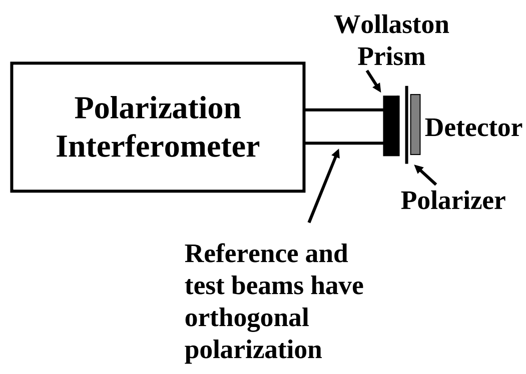

Pixelated Phase Sensor

- **Compacted pixelated array placed in front of detector**
- **Single frame acquisition**
  - **High speed and high throughput**
- **Achromatic**
  - **Works from blue to NIR**
- **True Common Path**
  - **Can be used with white light**

Use polarizer as phase shifter

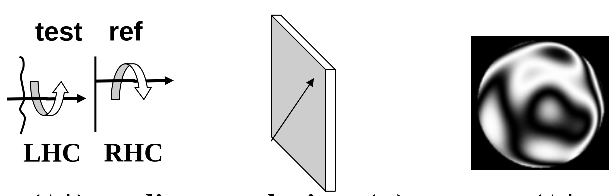

Circ. Pol. Beams ($\Delta\phi$) + linear polarizer (α) $\longrightarrow$ cos ($\Delta\phi + 2\alpha$)

Phase-shift depends on polarizer angle

Array of oriented micropolarizers

Polarizer array Matched to detector array pixels

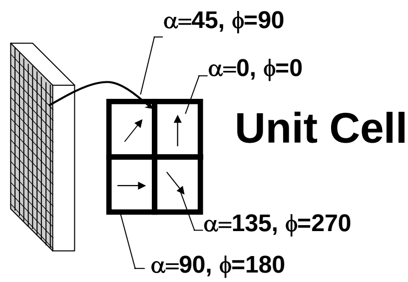

Electron micrograph of wire grid polarizers

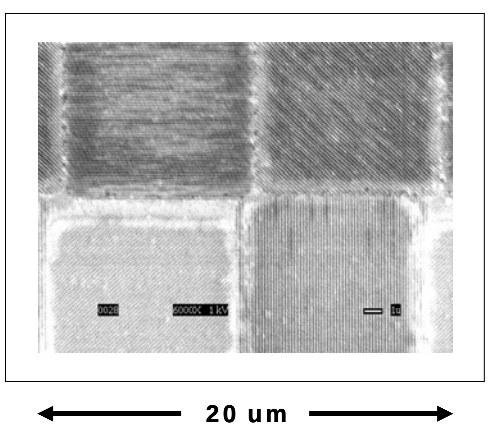

Array of phase-shift elements unique to each pixel

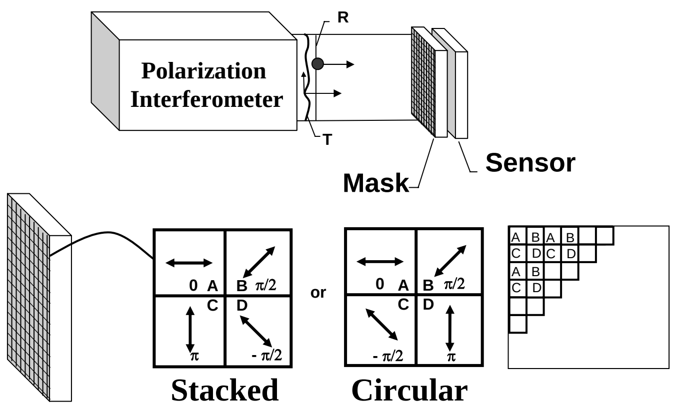

Phase error vs fringe tilt

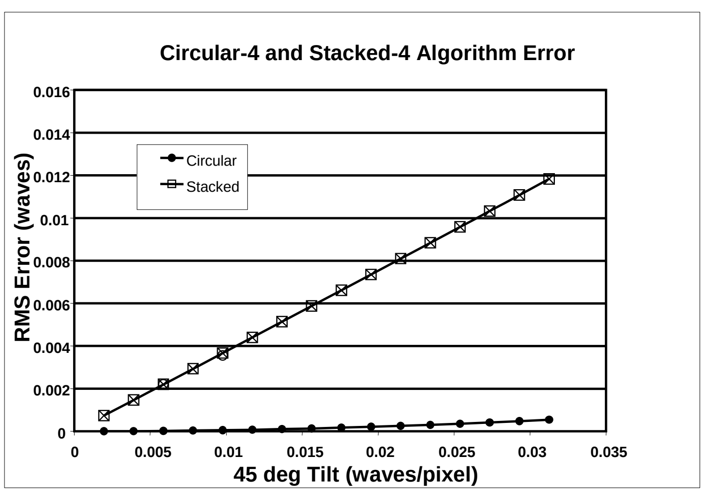

Calculation of phase using 3 x 3 element array

0	$\frac{\pi}{2}$	0	$\frac{\pi}{2}$
$-\frac{\pi}{2}$	1 π	2 $-\frac{\pi}{2}$	3 π
0	4 $\frac{\pi}{2}$	5 0	6 $\frac{\pi}{2}$
$-\frac{\pi}{2}$	7 π	8 $-\frac{\pi}{2}$	9 π

$$Tan[\theta_5] = \frac{2(I_2 + I_8 - I_4 - I_6)}{-I_1 - I_3 + 4I_5 - I_7 - I_9}$$

System Configuration

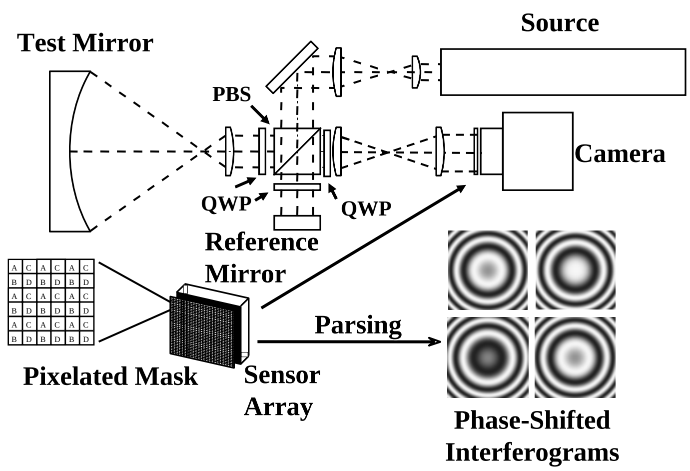

Measurements

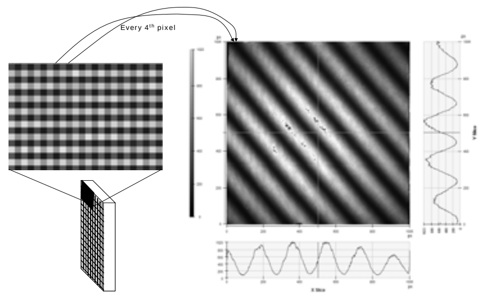

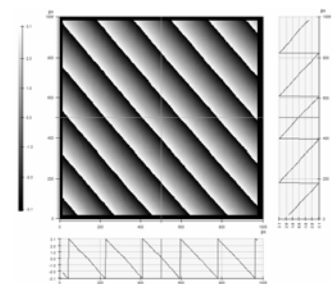

Fringe pattern synthesized by selecting every fourth pixel.

Phase map.

Measurement of 300 mm diameter, 2 meter ROC mirror

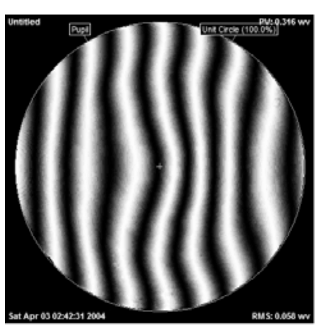

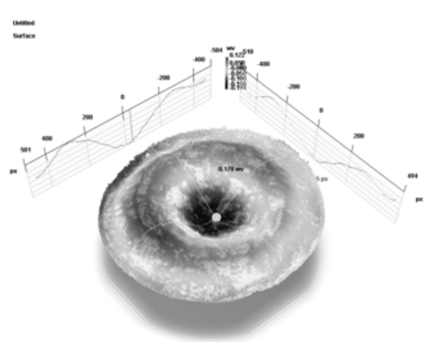

Mirror and interferometer on separate tables!

Measurement Results

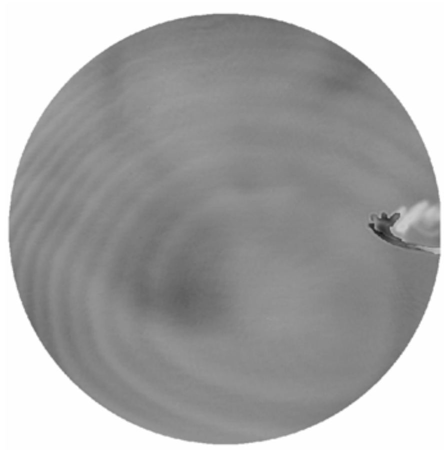

Air burst
Phase w/reference subtraction

Heat Waves from Hot Coffee

OPD

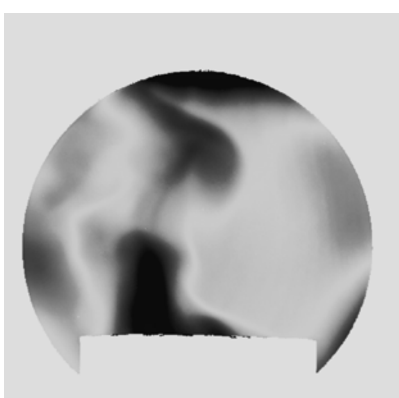

Slope

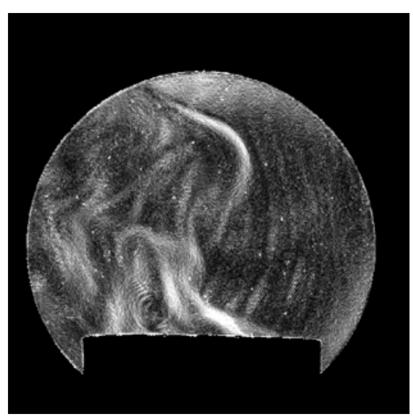

Simultaneous Phase-Shifting Fizeau – Tilt Between Reference and Test (Two Source Beams)

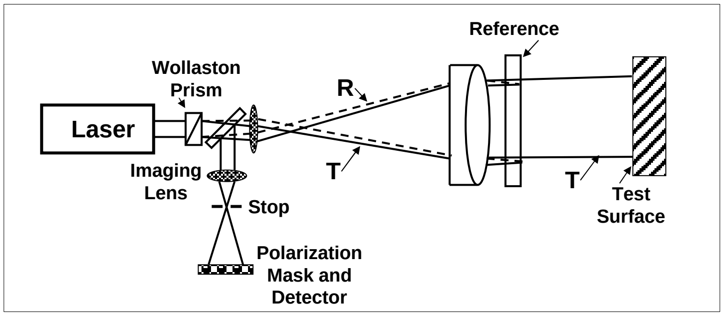

T and R have orthogonal polarization.

R reflected off reference and T reflected off test surface are nearly parallel and give the interference fringes.

Simultaneous Phase-Shifting Fizeau – Tilt Between Reference and Test

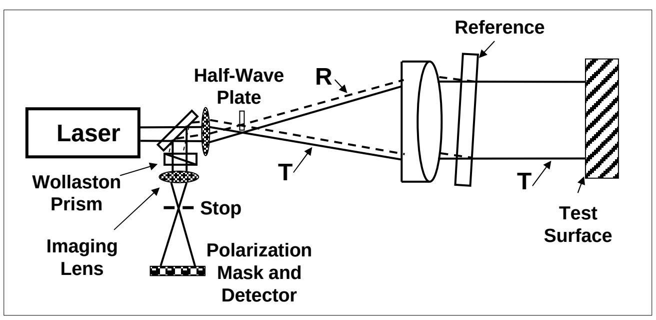

R reflected off reference and T reflected off test surface are tilted with respect to each other.

Half-wave plate makes polarization of reflected R orthogonal to reflected T.

Wollaston prism make T and R nearly parallel.

Simultaneous Phase-Shifting Fizeau – Short Coherence Length Source

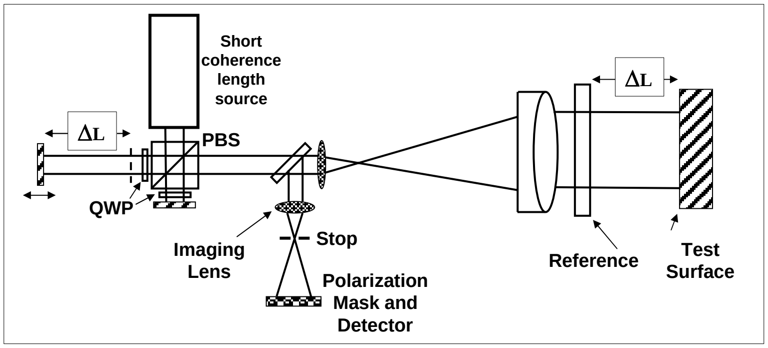

Interference pattern resulting from long path length source beam reflected off reference and short path length source beam reflected off test surface.

Test and reference beams have orthogonal polarization.

Fewer spurious fringes.

Simultaneous Phase-Shifting Fizeau – Short Coherence Length Source – Testing Windows

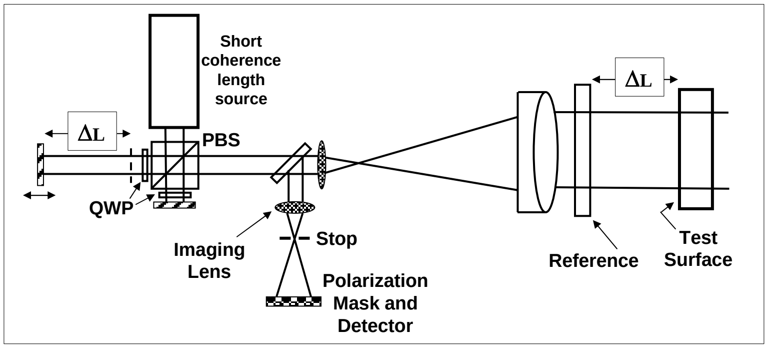

Testing window surfaces that are nearly parallel.

Test and reference beams have orthogonal polarization.

Interference Fringes Obtain Testing a Thin Glass Plate

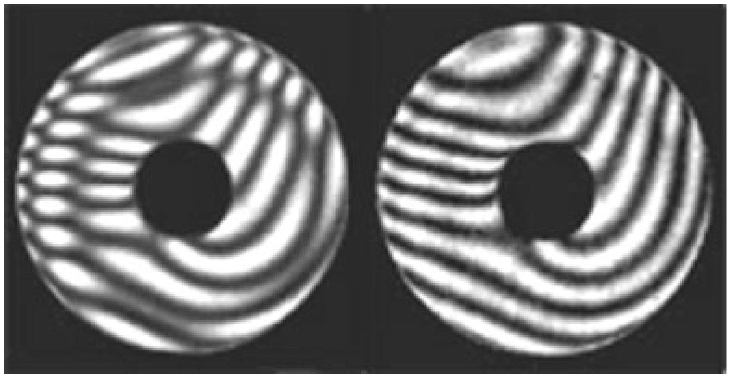

a) Long coherence length source | b) Short coherence length source

Pixelated Phase Sensor Advantages

• Single frame acquisition
  - High speed and high throughput
•Achromatic
  – works from blue to NIR
• True Common Path
  – Can be used with white light
• Fixed Carrier
  – Faster processing and calib.
• Compact
  – no bigger than camera
• Versatile
  – can be interfaced to many interferometer configurations

Multiple Wavelength and Vertical Scanning Interferometry

- White Light Interferometry eliminates ambiguities in heights present with monochromatic interferometry
- Techniques old, but use of modern electronics and computers enhance capabilities and applications

How High is the Step?

Steps > $\lambda/4$ between adjacent detector pixels introduce integer half-wavelength height ambiguities

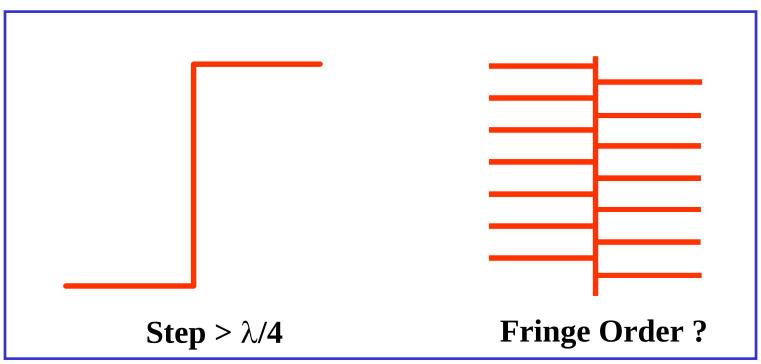

Interferograms of Diffraction Grating

Red Light

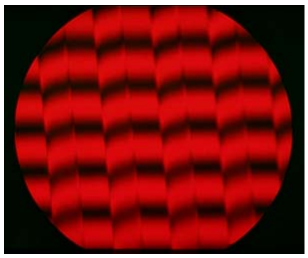

White Light

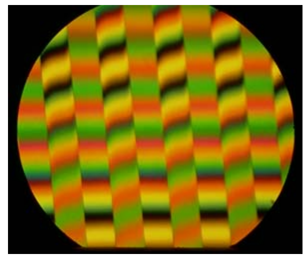

Profile

Two Wavelength Measurement

- Measure Beat Frequency
- Long Effective Wavelength

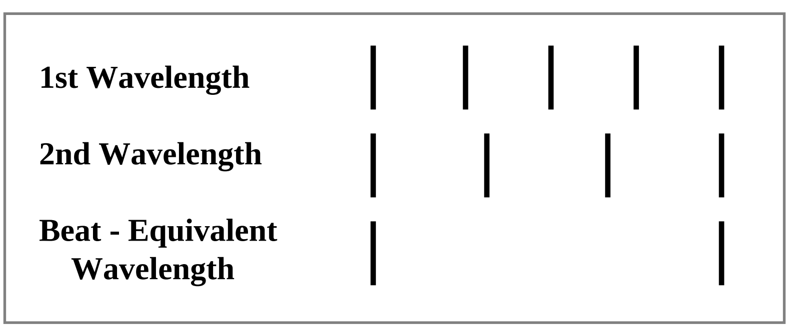

Two Wavelength Calculation

Equivalent Wavelength $$\lambda_{\mathbf{eq}} = \frac{\lambda_1 \lambda_2}{|\lambda_1 - \lambda_2|}$$

Equivalent Phase $$\varphi_{\mathbf{eq}} = \varphi_1 - \varphi_2$$

No height ambiguities as long as height difference between adjacent detector pixels < equivalent wavelength / 4

Diffraction Grating Measurement

Single wavelength (650 nm)

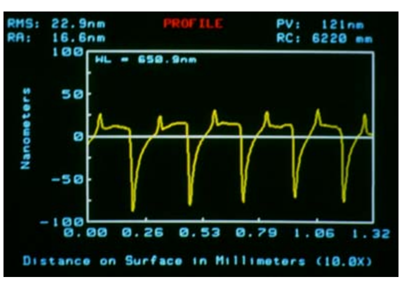

Equivalent wavelength (10.1 microns)

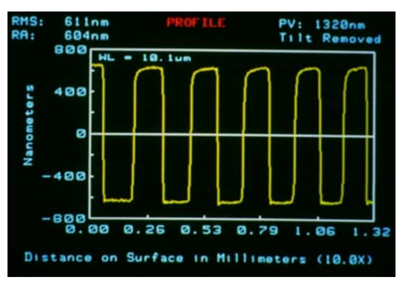

3-D Two-Wavelength Measurement (Equivalent Wavelength, 7 microns)

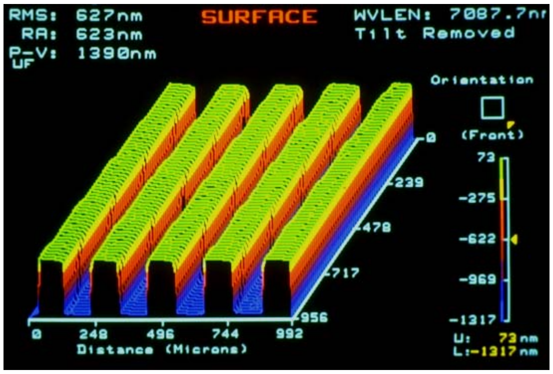

Two-Wavelength Measurement of Step

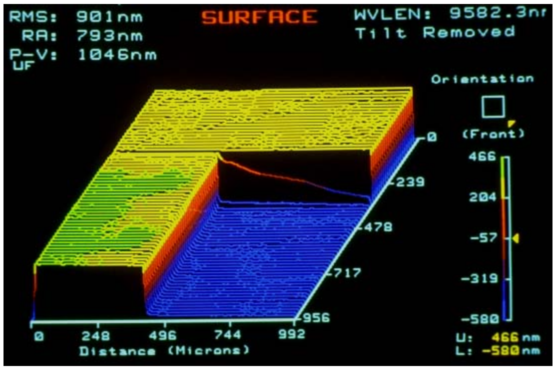

Wavelength Correction

Compare

- Heights calculated using equivalent wavelength
- Heights calculated using single wavelength

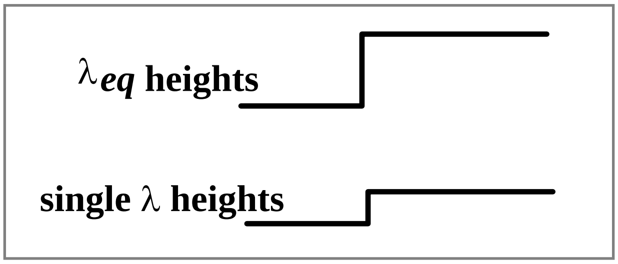

Add N x $\lambda/2$ to heights calculated using single wavelength so difference < $\lambda/4$

Wavelength Correction Measurement of Step

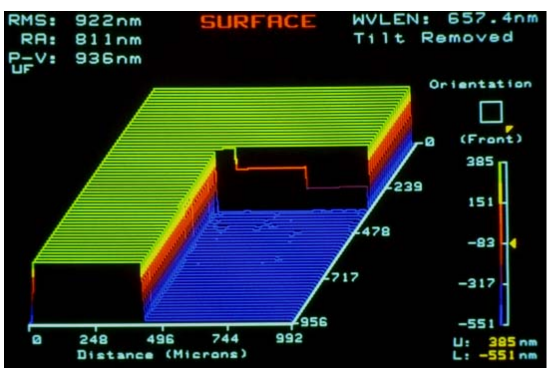

White Light Interference Fringes

- Fringes form bands of contour of equal height on the surface with respect to the reference surface.
- Fringe contrast will be greatest at point of equal path length or "best focus."

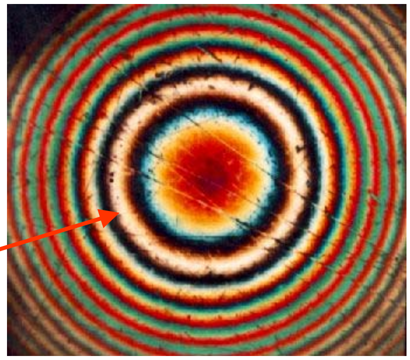

Principles of Vertical Scanning Interferometry

- A difference between the reference and test optical paths causes a difference in phase
- Best fringe contrast corresponds to zero optical path difference
- Best focus corresponds to zero optical path difference

Interference *Microscope Diagram*

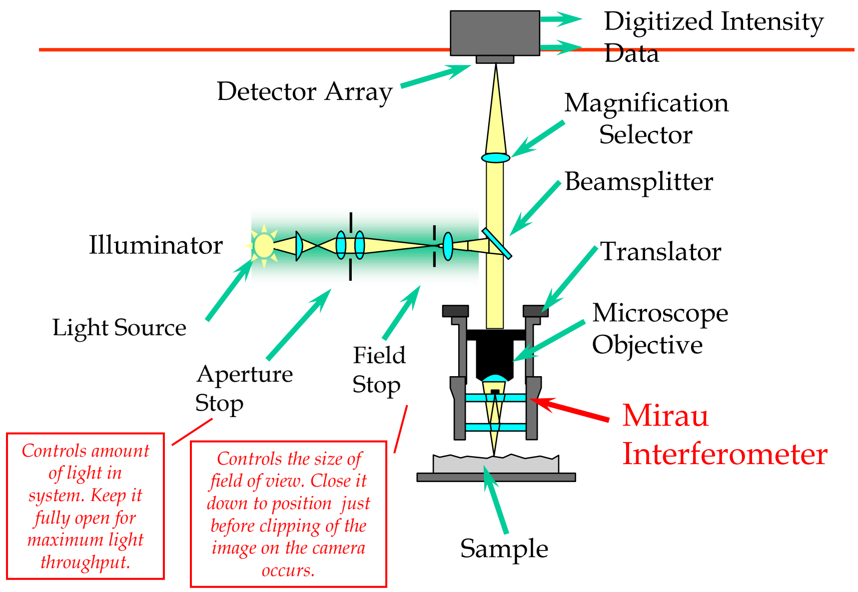

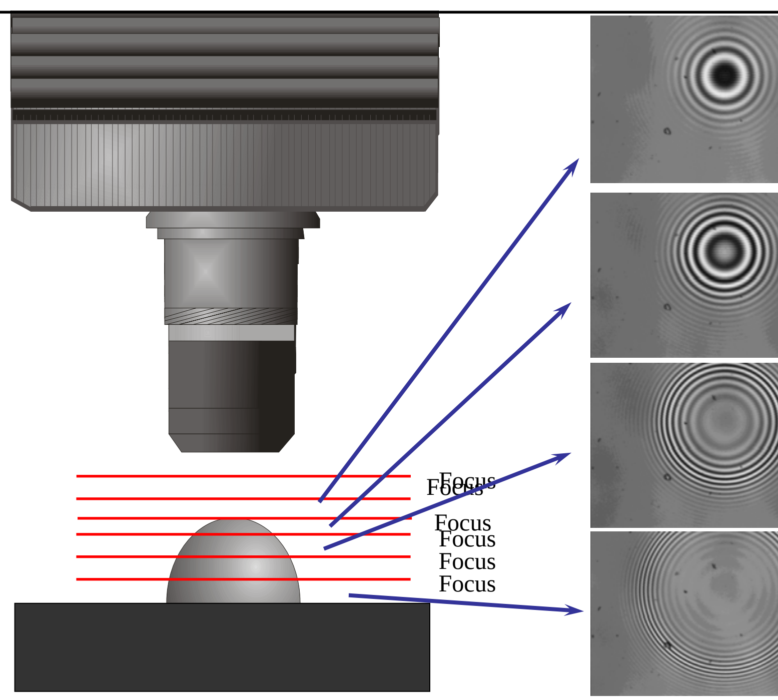

Typical White Light Fringes for Stepped Surfaces

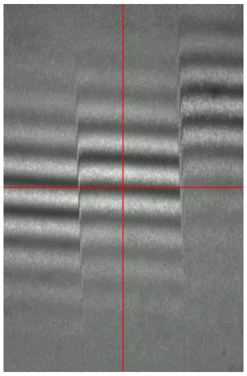

Fringes

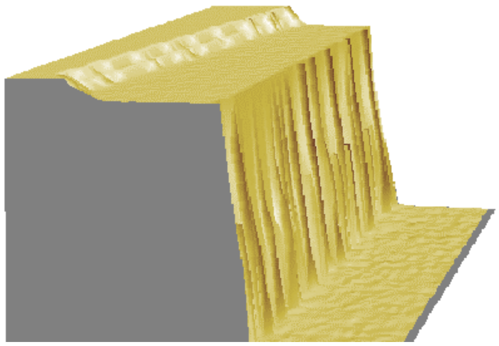

Phase map

Vertical Scanning Interferometer VSI

White Light Interferograms

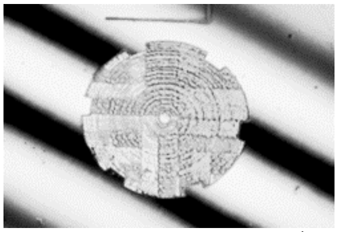

Focus Position A

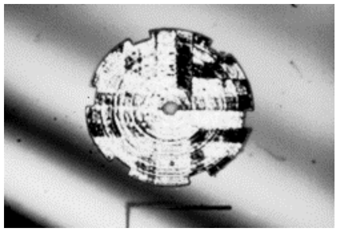

Focus Position B

As the scan moves different areas of the part being measured come into focus (have zero OPD or maximum contrast between fringes). A determination of the point of maximum contrast and knowledge of the motor position allows a reconstruction of the surface shape.

Intensity Signal Through Focus

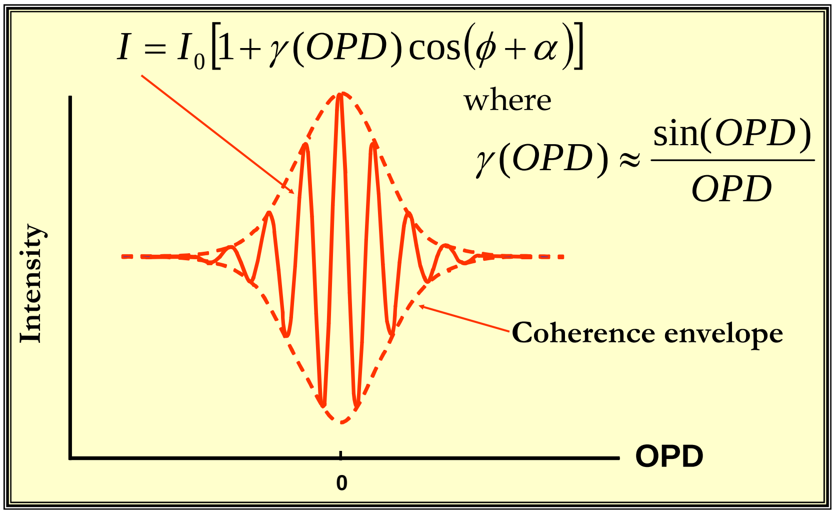

Typical Instrument

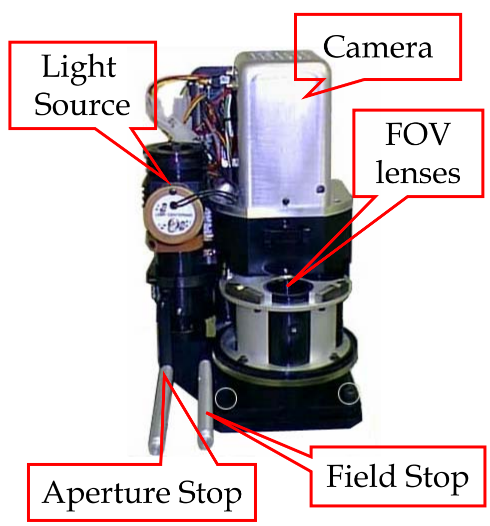

Stitched Measurement

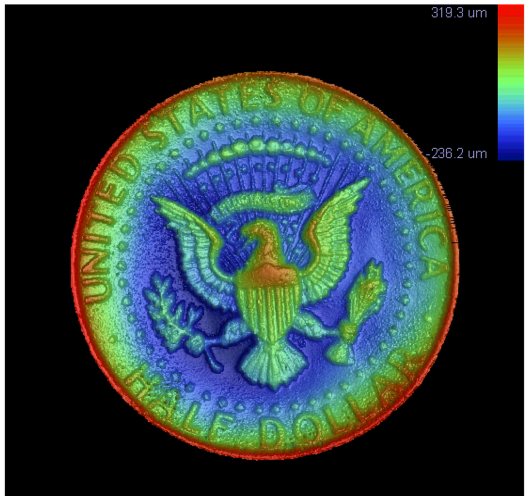

VSI mode

Step Measurement

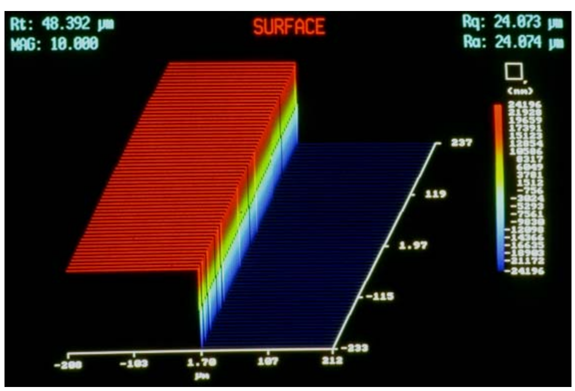

Print Roller

Print Roller Measurement

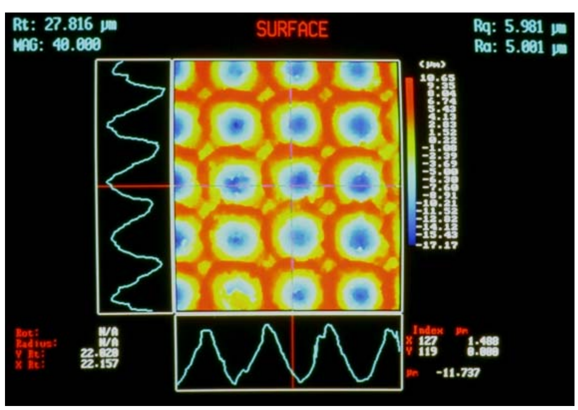

Paper Measurement

Micromachined Silicon Measurement

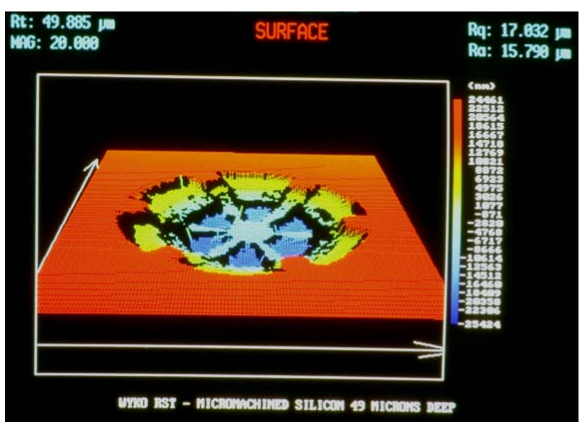

Binary Optic Lens

Surface Stats:

RMS: 561.30 nm

PV: 2.37 um

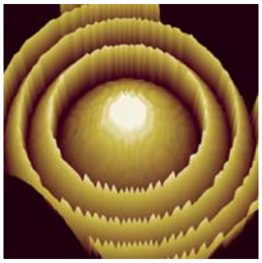

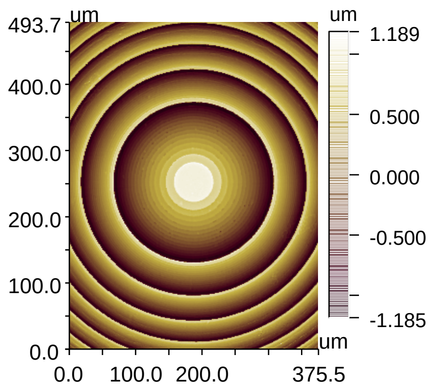

Chatter Seen on Camshaft

Surface Stats:

Rq: 872.06 nm

Ra: 693.90 nm

Rt: 7.47 um

Terms Removed:

Cylinder & Tilt

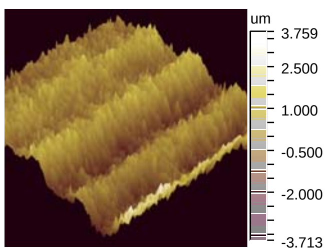

Heart Valve

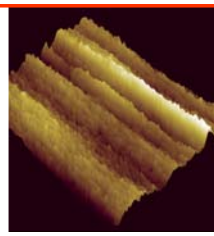

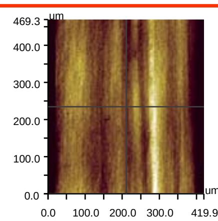

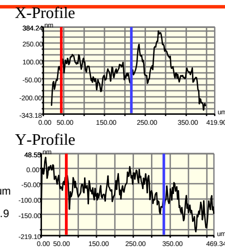

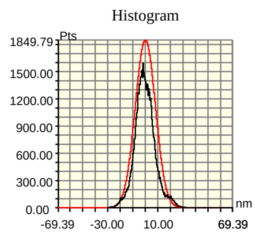

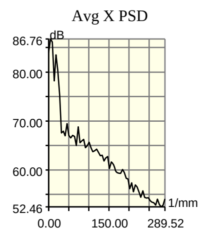

Data Statistics

Rt: 1.419 um

Ra: 87.391 nm

Rq: 113.942 nm

Pits in Metal

Mag: 10.0 X
Size: 248 X 239
Sampling: 1.70 um
Mode: VSI

Surface Stats:

Rq: 5.07 um
Ra: 3.44 um
Rt: 31.05 um

Terms Removed:

Tilt

Surface Data